Hierarchical Control for Voltage Harmonics Compensation in Multi-Area Microgrids

Hashempour, Mohammad M.; Savaghebi, Mehdi; Quintero, Juan Carlos Vasquez; Zapata, Josep Maria Guerrero

Published in:
Proceedings of the 2015 IEEE 10th International Symposium on Diagnostics for Electrical Machines, Power Electronics and Drives (SDEMPED)

DOI (link to publication from Publisher):
10.1109/DEMPED.2015.7303723

Publication date:
2015

Document Version
Early version, also known as pre-print

Hierarchical Control for Voltage Harmonics Compensation in Multi-Area Microgrids

Mohammad M. Hashempour, Mehdi Savaghebi, *Member, IEEE*, Juan C. Vasquez, *Senior Member, IEEE*, and Josep M. Guerrero, *Fellow, IEEE*

***Abstract* — In this paper, the power quality of multi-area microgrids is addressed. For this, Active Power Filters (APFs) and Distributed Generators (DGs) inverters are used. To achieve the reference value of power quality indices of different areas, a strategy based on cooperation between DGs and APFs is proposed. Hierarchical control is applied to control DGs inverters and APFs in a coordinated way. Primary control consists of power droop controller of DGs, selective virtual impedance and voltage/current regulators. Based on the secondary control, voltage compensation of Points of Common Coupling (PCCs) of multi-area microgrid is carried out by DGs. Voltage compensation of PCCs by DGs may cause violation from maximum allowable voltage distortion at DGs terminals. Thus, tertiary control is used to mitigate these violations by using APF in proper coordination with secondary control. Evaluation of the proposed hierarchical control is carried out by simulation.**

***Index Terms* — Active Power Filter, Distributed Generator (DG), Hierarchical Control, Multiple Voltage Harmonic Compensation, Multi-Area Microgrid.**

I. Introduction

COMBINATION of Distributed Generators (DGs), energy storages and loads in a small-scale grid is called Microgrid. Microgrids may operate as connected to main grid (grid-connected) or isolated from that (islanded). DGs are usually connected to microgrids by power electronic interface converters. To regulate voltage/frequency at DGs terminals, proper control of the interface inverters is recommended [1], [2]. Some strategies based on control of DGs inverters have been suggested for improving power quality of microgrids. Some of them address voltage harmonic compensation [3]-[5]. In this line, the present paper considers voltage harmonic compensation of islanded microgrids.

Voltage Control Method (VCM) with the help of a single-phase DG is used in [3] to compensate voltage harmonics of PCC. Control strategy of [4] is based on selective voltage harmonic compensation. In this method, different rated power of each DG is considered for compensation effort control. Despite significant voltage improvement of PCC in this method, output voltages of DGs can be significantly distorted.

To tackle this problem, an effective method has been suggested in [5] to achieve desirable power quality at PCC and DGs terminals with the help of APFs. The coordination between DGs and APFs is based on voltage THD at DGs terminals and inverters nominal power. According to [5], in case of multiple APFs, utilizing APFs is simultaneous and compensation sharing between them is based on their rated power. However, applying several APFs at the same time is not economic. Moreover, in this method the coordination is between APFs and all DGs, whereas to reduce power losses and compensation effort of APFs, it might be better making coordination between APFs and the DGs that the violations are occurred for them.

Concerning compensation of voltage distortion at DGs terminals, the reference voltage quality index in [5] is set to $THD = 5\%$, however, sometimes it is needed to reduce voltage distortion less than this value and/or selectively mitigate voltage distortion of specific harmonic orders.

Considering the proliferation and geographical spread of DGs and sensitive loads, power quality of multi-area inverter-based microgrids is addressed in the present paper. Moreover, the proposed approach is able to resolve the aforementioned defects of [5] and to provide desired power quality for main buses of an islanded microgrid (PCC and DG buses).

II. Proposed Hierarchical Control Scheme

Fig. 1(a) shows the general microgrid topology. As it can be seen in this figure, microgrid is divided to several areas that each area includes at least one DG. The main distinction between the areas is the required voltage quality based on its load condition and topology. Parallel APF in each area compensates voltage harmonic distortion by proper injection of harmonic current. Therefore, based on each area voltage quality situation, necessity of parallel APF can be determined. It is shown in Fig. 1(a) that each area has two main bus categories: PCC and node(s). Considering possible sensitive loads at node(s), voltage quality of all PCCs and nodes should be taken into account.

The proposed method to improve power quality of microgrids is based on the hierarchical control as can be seen in Fig. 1(b). This figure shows the proposed hierarchical control structure for a typical area. Primary (Local) control includes power droop controller, selective virtual impedance and inner voltage and current controllers.

This work was supported by the Technology Development and Demonstration Program (EUDP) through the Sino-Danish Project "Microgrid Technology Research and Demonstration" (meter.et.aau.dk).

M. M. Hashempour is with the Department of Electrical Engineering, Karaj Branch, Islamic Azad University, Iran (e-mail: hashempourmehdi@gmail.com).

M. Savaghebi, Juan C. Vasquez and J. M. Guerrero are with the Department of Energy Technology, Aalborg University, Aalborg East DK-9220, Denmark (e-mail: mes@et.aau.dk, juq@et.aau.dk , joz@et.aau.dk).

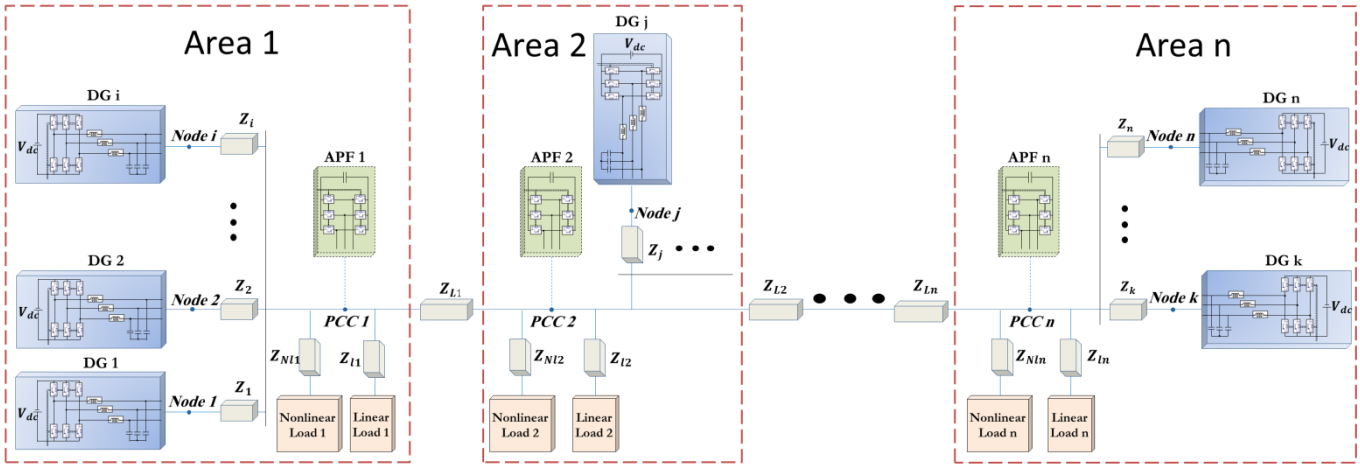

(a)

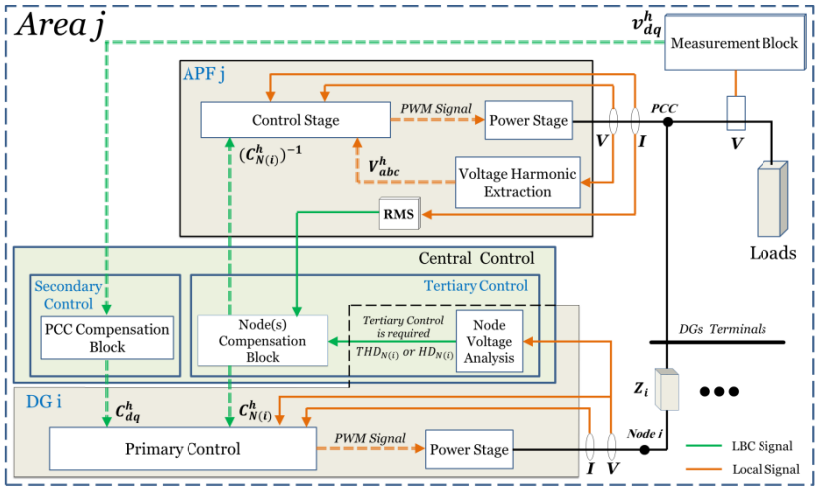

(b)

Fig. 1. General scheme of: (a) microgrid, (b) proposed control.

Secondary control is contrived for power quality improvement of PCC by DG(s). In fact, this control level estimates required compensation rate of PCC (C_{dq}^{h}) based on the data gathered by "Measurement Block" (v_{dq}^{h}). The estimated values are sent to local control of each DG. Due to compensation of PCC by DG(s), output voltage of DG(s), node (i) in Fig. 1(b), may become distorted [5]. Tertiary control is contrived to improve power quality of node(s). In this level, APF is used to cooperate with DG(s) for compensating PCC. By this, compensation rate of DG(s) is reduced and the node(s) voltage will be less distorted and overloading will not happen for DG(s) inverter. However, for some areas it might require providing higher power quality and/or mitigating specific voltage harmonics to reference values at node(s). In this case, voltage harmonics mitigation of node(s) to maximum allowable value will not be the only aim. On the other hand, in some load conditions using APF is not economic and it might be better to switch it off. In this situation, APF rated power should be considered, too. As a result, a coordinated control between APF rated power and voltage quality reference of node(s) should be designed for each area (see Fig. 1(b)). As it can be seen in Fig. 1(b), each area might include several DGs so APF is communicated with those that require voltage compensation in their nodes. As it can be seen in Fig. 1(b), secondary and tertiary controls are central controllers; meaning that they may be located far from APF and DG(s). In fact, communication between these levels and control stages of DG(s) and APF is accomplishable by Low Bandwidth Communication Link (LBCL).

Primary control contains power droop controller for sharing fundamental component of active/reactive powers, and virtual impedance for improving the load fundamental and harmonic components sharing among DGs [4]. It is obvious that in the areas with one DG, power and harmonic current sharing are not needed. Voltage and current loops are Proportional-Resonant (PR) controllers which tune Pulse Width Modulation (PWM) based on their reference values.

Fig. 2 shows compensation effort controller block. As can be observed in this figure, secondary and tertiary control related signals are applied in this controller to affect DG performance based on load conditions and voltage harmonic distortion in the microgrid. In fact, secondary control signal (C_{dq}^{h}) is for compensating PCC (by DG effort) and on the other side, tertiary control signal ($C_{N(i)}^{h}$) is for compensating the node(s) (by reducing DG effort in voltage harmonic mitigation of PCC). Note that these signals are determined based on the required voltage quality of PCC and the

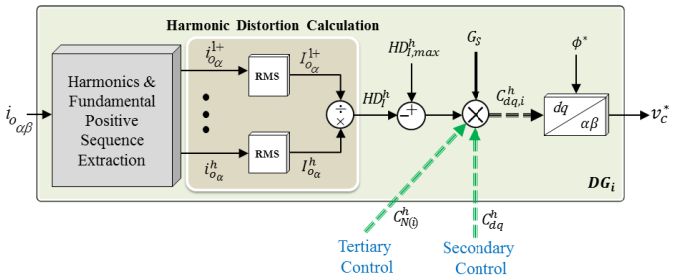

Fig 2. DGs compensation effort controller.

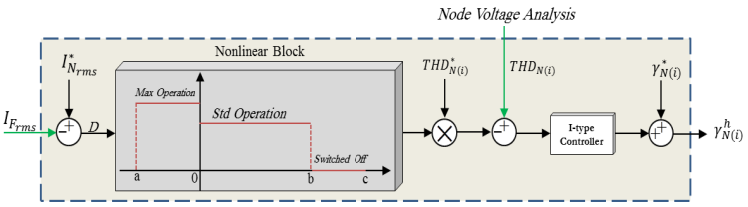

Fig. 3. Block diagram of $\gamma^h_{N(i)}$ calculation.

node(s), respectively (see Fig. 1(b)). It is worth noting that to reduce compensation effort of the DG(s) which needs tertiary control cooperation, $C^h_{N(i)}$ is just sent to the areas with several DGs. In other words, for the areas with single DG, PCC voltage distortion will be reduced by cooperation of APF with that DG based on the tertiary control. As a result, secondary control signal (C^h_{dq}) will be tuned automatically. More details about primary and secondary controls are available in [1], [2], [4], and [5].

III. Tertiary Control

Tertiary control manages the coordination between APF and DG(s) in order to compensate PCC while the required voltage quality of node(s) is achieved. The general approach for designing control stage of APF can be found in [6] and the strategy for fixing APF dc-link is extracted from [7]. APF causes voltage harmonics of:

$$V^h_{N(i)} = V^h_{N0} + Z^h_{N(i)} I^h_F \quad (1)$$

at PCC and reduces voltage harmonic distortion of node(s). In Eq. (1), V^h_{N0} is the voltage vector of i-th node without any compensation, $Z^h_{N(i)}$ is impedance matrix and I^h_F is injected harmonic current to PCC by APF. Since the compensation of node(s) is carried out by injecting harmonic current to PCC, the impedance between these two points (Z_n in Fig. 1(a)) should be taken into account in impedance matrix. I^h_F can be represented by the following equation:

$$I^h_F = \gamma^h_{N(i)} V^h_{N(i)} \quad (2)$$

where $\gamma^h_{N(i)}$ is the current gain of APF. Based on Eqs. (1) and (2), the following equation can be extracted for harmonic voltage produced by APF at PCC:

$$V^h_{N(i)} = -(C^h_{N(i)})^{-1} V^h_{N0} \quad (3)$$

where:

$$C^h_{N(i)} = Z^h_{N(i)} \gamma^h_{N(i)} - E \quad (4)$$

$C^h_{N(i)}$ is coordination coefficient that is distinctive for individual harmonics. Again, due to compensation of PCC with the aim of voltage harmonic compensation of node(s), $C^h_{N(i)}$ should change until the reference voltage quality of node(s) is achieved (regardless of $V^h_{N(i)}/V^h_{N0}$ ratio). In fact, as it is shown in Eq (4), $C^h_{N(i)}$ is dependent on $\gamma^h_{N(i)}$.

Fig. 3 shows the strategy of calculating $\gamma^h_{N(i)}$. As can be seen in this figure, two parameters are important in this calculation: node voltage distortion rate (transferred from "Node Voltage Analysis" block) and the rms value of APF output current ($I_{F_{rms}}$). In Fig. 3, $I^*_{N_{rms}}$ is the rms value of APF nominal current. The difference between $I^*_{N_{rms}}$ and $I_{F_{rms}}$, that is represented by D, is transferred to "Nonlinear Block". Based on this block, three levels are defined for APF compensation effort. If $D < 0$, nonlinear block increases the reference value of *THD* in i-th node ($THD^*_{N(i)}$) to its maximum allowable value (that can be 5% according to IEEE Standard 519 [8]) to reduce APF compensation effort and prevent APF overloading. On the other hand, using APF for compensating low range of voltage distortion ($b < D < c$) is not economic enough, therefore, as it is shown in Fig. 3, nonlinear block switches off the APF in this situation. After determination of $THD^*_{N(i)}$ based on nonlinear constraint, an integrator controller is used to tune $\gamma^h_{N(i)}$ to achieve $THD^*_{N(i)}$ in i-th node. It is worth noting that $\gamma^*_{N(i)}$ is designed for making a droop scheme. However, to use coordination coefficient in APF and DG(s) control stages, $\gamma^*_{N(i)}$ is adjusted so that we have $0 < C^h_{N(i)} < 1$. By this, no compensation of node(s) is corresponding to $C^h_{N(i)} \sim 1$ and complete voltage harmonic compensation is corresponding to $C^h_{N(i)} \sim 0$ (although $C^h_{N(i)} \sim 0$ is impractical due to nonlinear block constraint and the reference voltage quality of node(s)). Note that according to the reference voltage quality of nodes in different areas, tertiary control can be tuned based on voltage harmonic distortion rate ($HD_{N(i)}$) instead of $THD_{N(i)}$ (see Fig. 1(b)). As it is shown in Fig. 1(b), $C^h_{N(i)}$ is sent to primary control of DG(s) and $(C^h_{N(i)})^{-1}$ is sent to APF control stage. It is noteworthy that by reducing the voltage distortion of node(s), interface inverter current will be reduced, too.

IV. Simulation Results

The test microgrid is shown in Fig. 4. To evaluate proposed hierarchical control in different areas and load conditions, three areas with different voltage quality requirement for the nodes as well as PCCs are considered in the microgrid. To avoid voltage harmonic propagation between areas and provide high power quality for the loads in PCCs, voltage quality requirement of PCCs is set to higher levels than that of nodes (reference value HD^*_{PCCs} =0.5% for PCCs). It is worth noting that compensation of 5th and 7th harmonics (the main orders) of nodes and PCCs voltages are dealt with in this paper. The parameters of APFs power stages and distribution and inter-

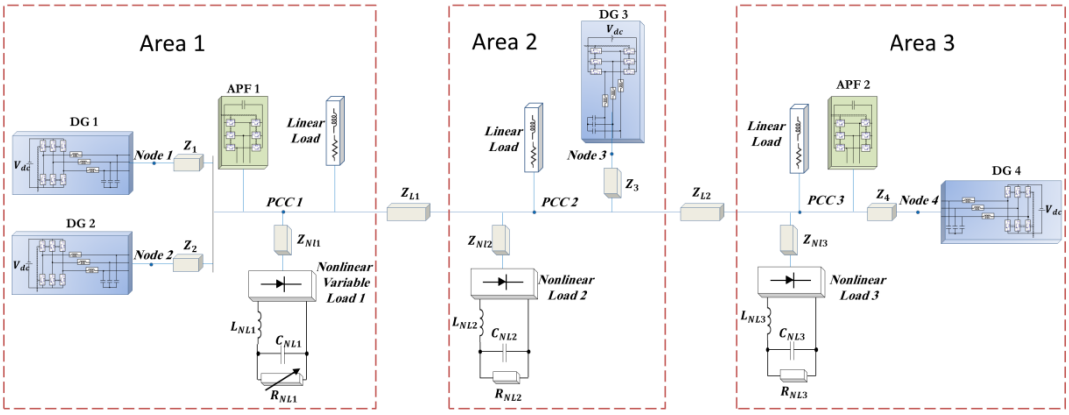

Fig. 4. Test system.

-area lines are available in Table I. Moreover, APFs and tertiary control parameters are represented in Table II.

The data concerning primary and secondary controls can be found in [4]. Based on DGs power droop characteristics, DG4 rating is twice of DG1 and DG3 rating is quadruplicate of DG2. To test different parts of the proposed hierarchical control, clearly, Table III shows simulation process and the following explanations are based on this table. It is worth noting that to extract voltage/current harmonic components, MSOGIFLL extraction method [9] is used and THD calculation way is according to [5]. MATLAB/Simulink is used for evaluating the proposed hierarchical control. Simulation results for each area are represented as follows.

TABLE I
TEST SYSTEM PARAMETERS

Area 1								
APF1 Power Stage		Distribution Lines			Nonlinear Load1			Linear Load
L_F (mH)	C_F (μF)	Z_1 (Ω-mH)	Z_2 (Ω-mH)	Z_{Nl1} (Ω-mH)	C_{NL1} (μF)	R_{NL1} (Ω)	L_{NL1} (mH)	Z_{L1} (Ω-mH)
20	2000	0.2-3.6	0.1-1.8	0.2-3.2	235	30-85-260	0.084	50-20
Aria 2								
Distribution Lines		Nonlinear Load2						Linear Load
Z_3 (Ω-mH)	Z_{Nl2}(Ω-mH)	C_{NL} (μF)	R_{NL} (Ω)	L_{NL} (mH)				Z_L (Ω-mH)
0.2-3.6	0.2-3.2	235	140	0.084				120-25
Area 3								
APF2 power stage		Distribution Lines		Nonlinear load3				Linear load
L_F (mH)	C_F (μF)	Z_4 (Ω-mH)	Z_{Nl3} (Ω-mH)	C_{NL} (μF)	R_{NL} (Ω)	L_{NL} (mH)		Z_L (Ω-mH)
20	2000	0.1-1.8	0.2-3.2	235	35	0.084		50-20
Inter-Area Lines								
Z_{L1} (Ω-mH)				Z_{L2} (Ω-mH)				
0.25-4.5				0.2-3.6				

TABLE II
CONTROL PARAMETERS

APFs Capacitor PI Controller			
K_p		K_i	
0.16		0.02	
Tertiary Control			
Area 1		Area 3	
I-Controller (K_i)	$\gamma^h_{N(1)}$	I-Controller	$\gamma^h_{N(2)}$
3.5e-3	4e-3	9e-4	2e-3
Nonlinear Block			
a	b	c	
Negative Value	1.25	2	

A. Area1 Simulation Results

Two DGs are in this area, so power and harmonic current sharing should be considered. It is assumed that voltage quality reference of the nodes is $THD^*_{N(1,2)}$ =3.5%. Remember that the reference voltage distortion index of PCCs is HD^*_{PCCs} =0.5%. As it is shown in Fig. 4, nonlinear load 1 is defined to be variable to test the proposed hierarchical control in a wide range of voltage harmonic distortion. Fig. 5 shows voltage harmonic distortion of the nodes 1&2 and PCC1 based on Table III time periods. As it is shown in this figure, due to harmonic current sharing between DGs, the nodes 1&2 and PCC1 voltages are distorted. This distortion is more severe in PCC1 due to voltage drop that is produced through $Z_{1\&2}$. It can be seen in this figure that voltage quality reference of PCC1 is achieved when secondary control is applied but node 1 voltage is distorted severely that is due to high harmonic current at this point. It shows that DG1 plays an important role in compensation of PCC1. Due to violation from reference quality at node 1 (that is shown in Fig. 6), tertiary control is required to mitigate node 1 voltage distortion to its reference value. However, due to harsh nonlinear load 1 (with R_{NL1} =30Ω), APF1 should tolerate a great effort for this aim. To reach $THD^*_{N(1)}$ =3.5% by tertiary control, APF1 should inject $I_{F_{rms}} > I^*_{N_{rms}}$ that means $D < 0$ based on Fig. 7 (note that in Fig. 7, in period $6< t <8$, D curve shows $I^*_{N_{rms}} - I_{F_{rms}}$ in situation that the reference voltage quality of nodes 1&2 is $THD^*_{N(1,2)}$ =3.5%). As a result and based on "Nonlinear Block" constraint, $THD^*_{N(1)}$ is changed from 3.5% to 5% (see Fig. 6). Note that a little deviation from the reference value of *HD5* in PCC1 by initiation of tertiary control (see Fig. 5) is for very high value of this parameter and the incoordination between PI controller of secondary control and I-controller of tertiary control. Remember that compensation of nodes (by tertiary control) is carried out by reduction of DGs efforts in compensating PCCs (by secondary control). However, this deviation will be removed in a longer time period.

Based on Table III, since nonlinear load 1 is reduced in the next period (by increasing R_{NL1} from 30 to 85Ω), according to Figs. 3 and 7, APF1 is active in its standard operation while $THD^*_{N(1,2)}$ =3.5% is achieved (see Fig. 6). In the second reduction of nonlinear load 1 (Table III), it can be

TABLE III
SIMULATION TIME PERIODS

Time (s)	0 < t < 2	2 < t < 4	4 < t < 6	6 < t < 8	8 < t < 10	10 < t < 12	12 < t < 14
Area 1	Droop Control, Fundamental Power & Current Sharing	Non-fundamental Current Sharing	Secondary Control is added	Tertiary Control is added	The first reduction of Nonlinear Load 1	The second reduction of Nonlinear Load 1	Tertiary Control is disconnected
Area 2	Droop Control		Secondary Control is added				
Area 3	Droop Control		Secondary Control is added		Tertiary Control is added		

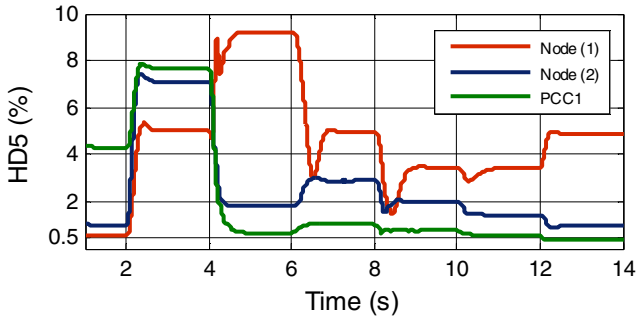

(a)

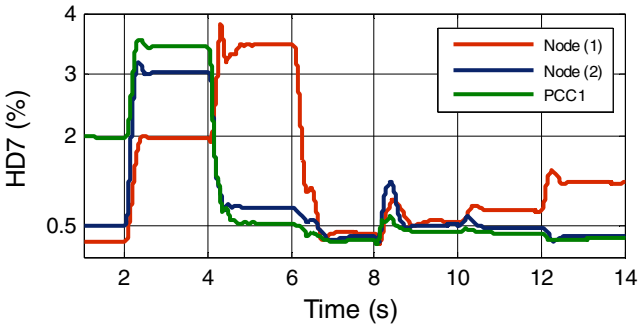

(b)

Fig. 5. Voltage harmonic distortion (Area1). (a) **5th** & (b) **7th** Harmonic.

seen in Fig. 6 that $THD^{*}_{N(1)}$ is nearly 5% without using tertiary control but by tertiary control, the reference voltage quality is achieved ($THD^{*}_{N(1)}$ =3.5%). However, as it can be seen in Fig. 7, APF1 is active in $b < D < c$; meaning that APF1 is used to compensate a low range of $V^{h}_{N(i)}$. It is not economic and may reduce APF1 effective lifetime. Consequently, according to the "Nonlinear Block" constraint of tertiary control, APF1 should be switched off and tertiary control should be disconnected. Based on Table III, this is happened in the final period. It can be seen that voltage harmonic distortion is increased, relatively (Fig. 5). Note that disconnecting APF is optional; meaning that this level might be removed in the case that lower value of $THD^{*}_{N(i)}$ is prior to economic issues.

As it can be seen in Fig. 6, node 1 voltage is significantly improved by tertiary control, but, node 2 voltage is a bit distorted that means DG2 effort in compensation of PCC1 is increased, relatively. This is for high inertia of I-controller in tertiary control in comparison with PI controller in the secondary level. However, $THD^{*}_{N(2)}$ is less than 3.5% in all the periods.

B. Area2 Simulation Results

In this area, the maximum allowable voltage distortion of node 3 is $THD^{*}_{N(3)}$ =5%. Since there is just a single DG in this area, power and harmonic current sharing is not considered. Fig. 8 shows voltage harmonic distortion of PCC2 and node 3 based on Table III time periods.

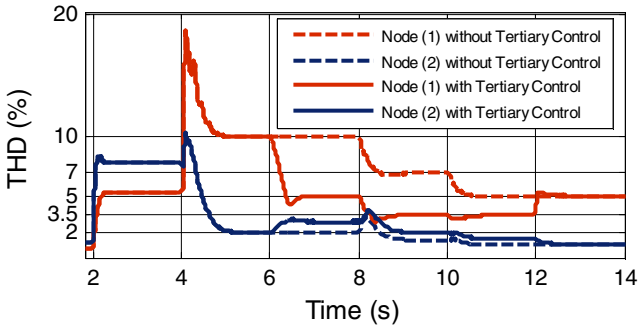

Fig. 6. THD of voltage (Area 1).

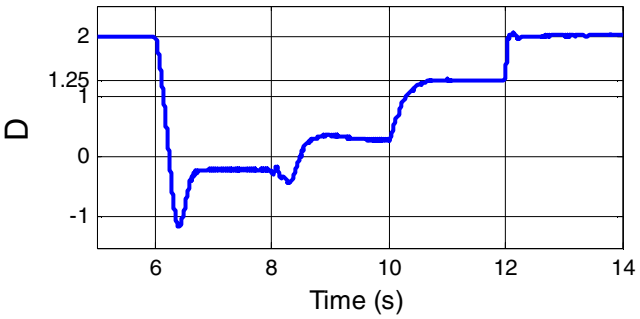

Fig. 7. D curve.

It can be seen that before secondary control, voltage distortion of node 3 is low, but, PCC 2 voltage distortion is high due to nonlinear load 2 and voltage drop that is produced through Z_3 (see Fig. 4). However, since secondary control is initiated, PCC2 voltage reference is achieved while node 3 voltage is distorted. Based on Fig. 9, $THD^{*}_{N(3)}$ is less than its maximum allowable value that means tertiary control is not required for this area. As a result, involvement of APF(s) in a multi-area microgrid can be determined by checking out node(s) voltage quality of individual areas.

Remember that PCCs voltages are almost distortion-free even though there is a bit of voltage harmonic propagation between areas. In fact, by increase of voltage distortion of PCCs due to current harmonic flow from neighbor area(s), secondary controllers increase DGs efforts for compensating PCCs voltages. This process is illustrated in Figs. 8 and 9, clearly. As can be seen in these figures, high power quality of PCC2 is achieved in all the periods, but, node 3 voltage is a bit distorted due to load condition of areas 1 and 3. It can be concluded that low harmonic current is flown to area 2 from areas 1 and 3 and it is compensated by secondary control of area 2.

A. Area3 Simulation Results

As it is represented in Fig. 4, there is just a single DG in this area, so, load sharing loops of primary control are eliminated from the hierarchical control. Voltage quality reference of PCC3 is like other areas, but, maximum allowable voltage distortion of node 4 is set to $HD^{5*}_{N(4)}$ =3.5%.

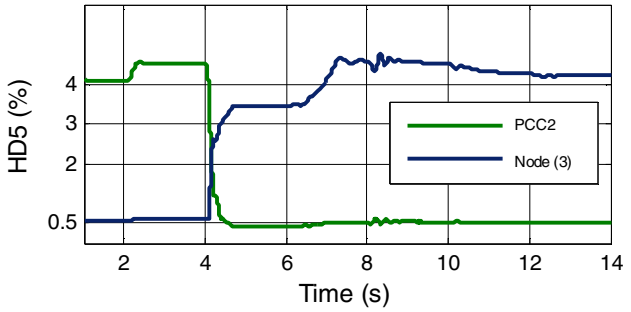

Fig. 8. Voltage harmonic distortion (Area 2).

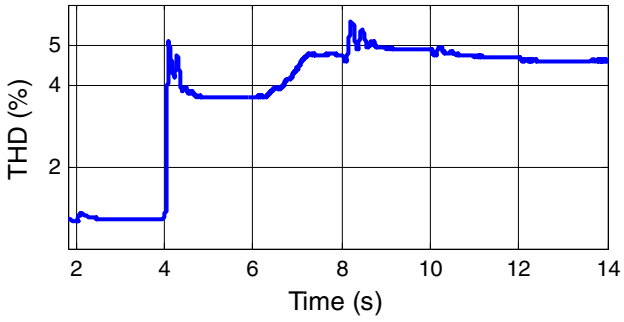

Fig. 9. Node (3) THD of voltage.

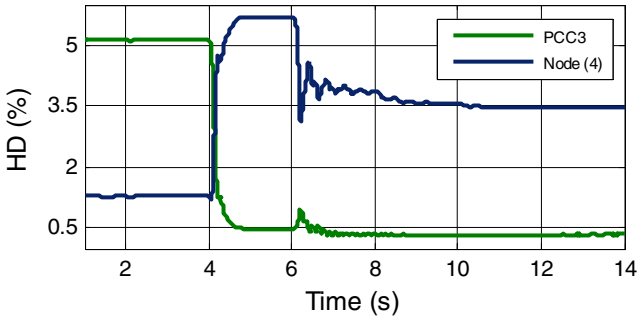

Fig. 10. Voltage harmonic distortion (Area 3).

According to Fig. 10, secondary control is accurate in achieving the quality reference of PCC3. However, it is observable in Fig. 10 that violation from node 4 maximum allowable voltage distortion is occurred, so, tertiary control is required. As it is represented in this figure, once the tertiary control is initiated, node 4 voltage quality is improved and the violation is eliminated. Since there is just one DG in area 3, the communication between tertiary and secondary levels lasts more than the areas with several DGs. In other words, control stages of area 3 (including APF2 and DG4 control stages) need more time to match with each other. This phenomenon becomes more obvious by comparing Figs. 5 and 10. In Fig. 5, there is almost no oscillation in the figure and reference voltage quality of different points of area 1 is achieved in a short time. In fact, it is because of sharing compensation among three compensators. However, according to Fig. 10, reference voltage quality of main points of area 3 is achieved in longer times and with some oscillations.

V. Conclusion

A hierarchical control scheme to improve power quality of a multi-area microgrid is proposed. Microgrid is divided into individual areas and the hierarchical control is applied for each area. In order to achieve voltage compensation of each area, no communication is necessary between the areas. The hierarchical structure includes three levels. In the primary control, power and harmonic current sharing based on each area topology is done. Secondary level compensates PCC of each area by controlling DG(s) inverters of that area. Compensation of PCC by DG(s) may cause voltage distortion at DG(s) terminal and overloading of the interface inverters. Thus, tertiary control is designed to help DG(s) in compensating PCC by proper utilization of APF. The coordination between tertiary and secondary levels is based on APF rated power and the required power quality of each DG terminal.

References

[1] J. M. Guerrero, P. C. Loh, M. Chandorkar, and T.-L. Lee, "Advanced control architectures for intelligent MicroGrids- part I: decentralized and hierarchical control," *IEEE Trans. Ind. Electron.*, vol. 60, no. 4, pp. 1254-1262, Apr. 2013.

[2] J. M. Guerrero, P. C. Loh, T.-L. Lee, and M. Chandorkar, "Advanced control architectures for intelligent microgrids—part II: power quality, energy storage, and AC/DC microgrids," *IEEE Trans. Ind. Electron.*, vol. 60, no. 4, pp. 1263-1270, Apr. 2013.

[3] J. He, Y. W. Li, and M. S. Munir, "A flexible harmonic control approach through voltage-controlled DG–grid interfacing converters," *IEEE Trans. Ind. Electron.*, vol. 59, no. 1, pp. 444-455, Jan. 2012.

[4] M. Savaghebi, A. Jalilian, J. C. Vasquez, and J. M. Guerrero, "Secondary control for voltage quality enhancement in microgrids," *IEEE Trans. Smart Grid*, vol. 3, no. 4, pp. 1893-1902, Dec. 2012.

[5] M. Savaghebi, M. M. Hashempour, and J. M. Guerrero, "Hierarchical coordinated control of distributed generators and active power filters to enhance power quality of microgrids," in *Proc. 55th Int. Scientific Conf. Power and Electrical Engineering of Riga Technical University (RTUCON)*, 2014, pp. 259-264.

[6] J. Tlustý, J. Škramlík, J. Švec, and V. Valouch, "Cooperative control of active power filters in power systems without mutual communication," *Mathematical Problems in Engineering*, vol. 2010, pp. 1-13, 2010.

[7] T. L. Lee, J. C. Li, and P. T. Cheng, "Discrete frequency tuning active filter for power system harmonics," *IEEE Trans. Power Electron.*, vol. 24, no. 5, pp. 1209-1217, May 2009.

[8] *IEEE Recommended Practice and Requirements for Harmonic Control in Electric Power Systems*, IEEE Standard 519-2014, 2014.

[9] P. Rodriguez, A. Luna, I. Candela, R. Mujal, R. Teodorescu, and F. Blaabjerg, "Multiresonant frequency-locked loop for grid synchronization of power converters under distorted grid conditions," *IEEE Trans. Ind. Electron.*, vol. 58, no. 1, pp. 127-138, Jan. 2011.